PROCEEDINGS A

royalsocietypublishing.org/journal/rspa

Research

Cite this article: Sharma BL, Mishuris G. 2020 Scattering on a square lattice from a crack with a damage zone. *Proc. R. Soc. A* **476**: 20190686. http://dx.doi.org/10.1098/rspa.2019.0686

Received: 15 October 2019
Accepted: 13 February 2020

Subject Areas:
applied mathematics, mathematical modelling, mechanics

Keywords:
diffraction, crack, damage zone, Wiener–Hopf method

Author for correspondence:
Gennady Mishuris
e-mail: ggm@aber.ac.uk

One contribution to a special feature 'Recent advances in elastic wave propagation' in memory of Peter Chadwick organized by Yibin Fu, Julius Kaplunov and Ray Ogden.

THE ROYAL SOCIETY PUBLISHING

Scattering on a square lattice from a crack with a damage zone

Basant Lal Sharma[1] and Gennady Mishuris[2]

[1]Department of Mechanical Engineering, Indian Institute of Technology Kanpur, Kanpur, India
[2]Department of Mathematics, Aberystwyth University, Aberystwyth, UK

BLS, 0000-0002-4968-9203; GM, 0000-0003-2565-1961

A semi-infinite crack in an infinite square lattice is subjected to a wave coming from infinity, thereby leading to its scattering by the crack surfaces. A partially damaged zone ahead of the crack tip is modelled by an arbitrarily distributed stiffness of the damaged links. While an open crack, with an atomically sharp crack tip, in the lattice has been solved in closed form with the help of the scalar Wiener–Hopf formulation (Sharma 2015 *SIAM J. Appl. Math.*, **75**, 1171–1192 (doi:10.1137/140985093); Sharma 2015 *SIAM J. Appl. Math.* **75**, 1915–1940. (doi:10.1137/15M1010646)), the problem considered here becomes very intricate depending on the nature of the damaged links. For instance, in the case of a partially bridged finite zone it involves a 2×2 matrix kernel of formidable class. But using an original technique, the problem, including the general case of arbitrarily damaged links, is reduced to a scalar one with the exception that it involves solving an auxiliary linear system of $N \times N$ equations, where N defines the length of the damage zone. The proposed method does allow, effectively, the construction of an exact solution. Numerical examples and the asymptotic approximation of the scattered field far away from the crack tip are also presented.

1. Introduction

Among other distinguished as well as popular works [1], Peter Chadwick made several contributions to the wave propagation problems in anisotropic models with different kinds of symmetries as well as those applicable to the theory of lattice defects [2–8]. His research into

© 2020 The Authors. Published by the Royal Society under the terms of the Creative Commons Attribution License http://creativecommons.org/licenses/by/4.0/, which permits unrestricted use, provided the original author and source are credited.

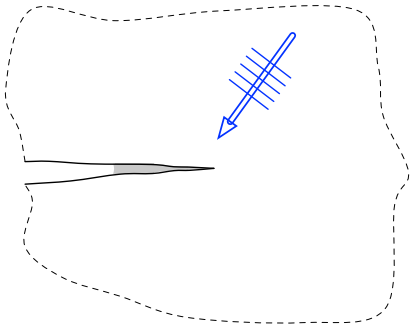

Figure 1. Schematic of an incident wave on a crack tip with damage. (Online version in colour.)

elastic cubic crystals is especially relevant in the context of the present paper as a discrete counterpart of a square lattice is natural when one considers waves interacting with a crack tip [9–14].

Indeed, the role of discrete models in the description of the mechanics and physics of crystals [15] and related structures has dominated studies of several critical phenomena, such as dislocation dynamics, dynamic fracture and phase transition, bridge crack effects, and resonant primitive, localized and dissipative waves in lattices among others [16–32]. The concomitant issues dealing with the propagation of waves interacting with stationary cracks and rigid constraints as well as surface defects have been explored in [12–14,33–42]. It is noteworthy that the continuum limit, which is a low-frequency approximation of the scattering problem for a single crack [13,43], recovers the well-known solution of Sommerfeld [44,45]. With respect to the crack-tip geometry, note that the discrete scattering problems have been solved in [12,13,35,38,40] for atomically sharp crack tips.

Typically, such situations of discrete scattering due to crack surfaces are further complicated as the crack tip is endowed with some structure, as shown schematically in figure 1, due to the presence of a cohesive zone, partial bridging of bonds, etc., commonly used in continuum mechanics [46–48]. The notion of a cohesive zone used in this paper is considered in a wider sense than in fracture mechanics (it does not clearly eliminate any singularities that do not arise in the discrete formulation). The zone simply emphasizes the fact that different links, subjected to a high-amplitude vibration, near the crack tip may undergo phase transition, damage and/or breakage at different times depending on the material's properties (manifesting by respective damage/fracture criteria [49]). As a result, a naturally created partial bridging and/or forerunning zone can be observed during crack propagation (e.g. [30,50]).

The problem considered in this paper, in fact, becomes much more intractable when compared with the scattering due to an atomically sharp crack tip that has been solved in [12,13] using the scalar Wiener–Hopf factorization [11,51]. As an example, it is shown that, in the case of a partially bridged finite zone, the corresponding Wiener–Hopf problem becomes vectorial as it involves a 2×2 matrix kernel that belongs to a formidable class [52–55]. In this paper, it is shown that a reduction to a scalar problem is possible with the additional clause that it involves solving an auxiliary linear system of $N \times N$ equations, where N represents the size of the cohesive zone. Such a reduction resembles the one proposed for the Wiener–Hopf kernel with exponential phase factors in the continuum case [52–55], and its recently investigated discrete analogue of scattering due to a pair of staggered crack tips [34,56]. It is also relevant to recall for such kernels an asymptotic factorization-based alternative, but approximate, approach [34,57].

Overall, the method proposed in this paper does allow, effectively, the construction of an exact solution, even in the general case of an arbitrary set of damaged links. The paper presents some numerical examples to demonstrate the effect of certain kinds of damaged links on the pattern of a scattered field. The expression obtained after an asymptotic approximation of the scattered field far away from the crack tip is also presented as a perturbation over and above that for the

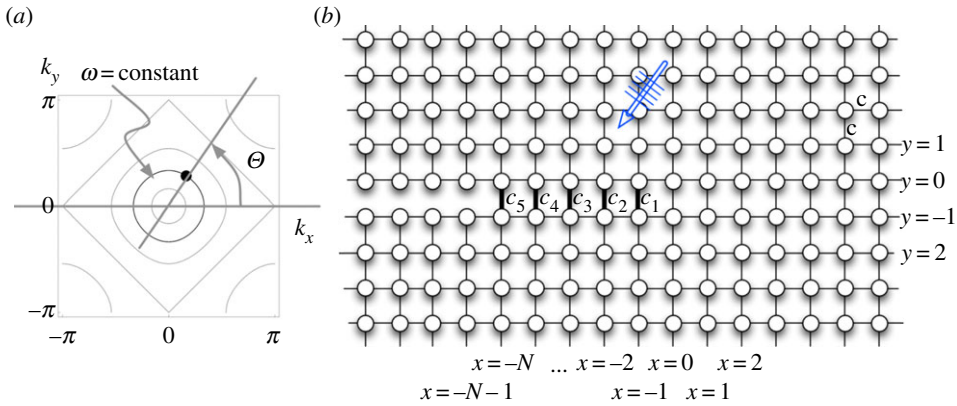

Figure 2. (*a*) Schematic of the incident wave parameters relative to the typical contours for a square lattice dispersion relation. (*b*) Geometry of the square lattice structure and the notation for the number of damaged sites $N = 5$. (Online version in colour.)

atomically sharp crack tip obtained earlier in [12]. A careful analysis of the continuum limit [43], in the presence of damaged links, which demands adoption of a proper scaling, is relegated to future work. The question of the behaviour of edge conditions with regard to sharp cracks [51,58] is anticipated to be crucial in such an exercise.

As a summary of the organization and presentation of the main aspects of this paper, §2 gives the mathematical formulation of the scattering problem. Section 3 provides the exact solution of the Wiener–Hopf equation modulo the reduced form to an auxiliary linear system of $N \times N$ equations. Section 4 presents some special scenarios of the distribution of the damaged links that allow either an immediate solution of the auxiliary equation or demonstrate the difficulty and richness of the problem by mapping its difficulty to a class of problems. Section 5 gives the far-field behaviour away from the crack tip as a perturbation in addition to that for a sharp crack tip, as well as some numerical examples. Section 6 concludes the findings of this paper. Appendix A gives the technical details of the application of the Wiener–Hopf method. For details of the theory of scattering and the Wiener–Hopf method, we refer to [51,59]; the mathematical aspects of convolution integrals and Fourier analysis can be found in [60–66]. For the issues dealing with the difficult cases of the matrix Wiener–Hopf problems, the reader is referred to [57,67–73].

2. Problem formulation

Let us consider a square lattice structure consisting of a semi-infinite crack that involves an additional structural feature near the crack tip. The bulk lattice is constructed with the same masses, m, situated at the points (x, y), $x \in \mathbb{Z}$, $y \in \mathbb{Z}$ and connected by elastic springs with stiffness, $c > 0$ (figure 1). The space coordinates are dimensionless and define the position of the corresponding mass $(x, y) = (\tilde{x}/a, \tilde{y}/a)$ (normalized by the length of the links between the neighbouring masses a). Displacement of the mass at each point is denoted as $u_{x,y}(t)$.

The bonded interface between the two half-planes consists of a finite segment of distributed springs of stiffness, $\{c_{-x}\}_{x=-1}^{-N}$ $(c_{-x} \geq 0)$, with connecting masses from the different sides of the interface attributed to the values of the variable x (figure 2). Note that some of the links can also be considered fully destroyed; thus, the geometry of the damage zone can be rather complex.

In the following, we will use the standard notation

$$\mathbb{Z}^+ = \{0, 1, 2, \ldots\}, \quad \mathbb{Z}^- = \{-1, -2, \ldots\} \quad \text{and} \quad \mathbb{Z} = \mathbb{Z}^+ \cup \mathbb{Z}^-. \tag{2.1}$$

We assume that an incident wave

$$u^i(x, y, t) = u^i_{x,y} e^{-i\omega t} = A e^{-ik_x x - ik_y y - i\omega t} \tag{2.2}$$

imposes the out-of-plane small deformation of the lattice. Here, $k_x, k_y \in \mathbb{R}$ are wavenumbers; also, sometimes we use $k_x = k\cos\Theta, k_y = k\sin\Theta$ with $k > 0$ and $\Theta \in [-\pi, \pi]$. The symbol $A \in \mathbb{C}$ is the complex dimensional amplitude of the wave. It is further assumed that $\omega = \omega_1 + i\omega_2$ (where $\omega_2 > 0$ is an arbitrary small number). The latter guarantees that the causality principle is addressed. Note that this implies $k = k_1 + ik_2$, where k_2 is small when ω_2 is small. We seek the harmonic solution to the problem of the form

$$u^t(x, y, t) = u^t_{x,y}\mathrm{e}^{-i\omega t} = (u^s_{x,y} + u^i_{x,y})\mathrm{e}^{-i\omega t}, \tag{2.3}$$

where $u^s_{x,y}$ and $u^i_{x,y}$ are the scattered part and the incident part, respectively.

The following set of equations are valid in each part of the lattice structure outside the interphase ($y \geq 1$ and $y \leq -2$):

$$c\Delta u_{x,y} + \omega^2 u_{x,y} = 0, \quad x \in \mathbb{Z}. \tag{2.4}$$

Here, Δ is the discrete Laplace operator with $\Delta u_{x,y} = u_{x+1,y} + u_{x-1,y} + u_{x,y+1} + u_{x,y-1} - 4u_{x,y}$ (see [11,12,74]) and in the following $u_{x,t} = u^t_{x,y}$.

The interphase consists of two lines $y = 0$ and $y = -1$ (figure 1). Let the damaged portion be denoted by the values of the coordinate x lying in

$$\mathcal{D} = \{-1, -2, \ldots, -N\}. \tag{2.5}$$

Let us denote the Kronecker delta by the symbol δ; it is equal to unity when $x \in \mathcal{D}$ and zero otherwise. Also we denote the discrete Heaviside function by $H(x)$ for $x \in \mathbb{Z}$, defined such that $H(x) = 1$ if $x \in \mathbb{Z}_+$, while $H(x) = 0$ when $x \in \mathbb{Z}_-$. Furthermore, let us introduce the notation

$$v_x = (u_{x,0} - u_{x,-1}), \quad v^{i,s}_x = (u^{i,s}_{x,0} - u^{i,s}_{x,-1}), \quad x \in \mathbb{Z}. \tag{2.6}$$

As a result, for $x \in \mathbb{Z}$, the conditions $c\Delta u_{x,0} + (c - c_{-x}\delta_{\mathcal{D},x} - cH(x))v_x + \omega^2 u_{x,0} = 0$ and $c\Delta u_{x,-1} - (c - c_{-x}\delta_{\mathcal{D},x} - cH(x))v_x + \omega^2 u_{x,-1} = 0$, linking the top part of the lattice with the bottom part, can be written as

$$c\Delta u^s_{x,0} + (c - c_{-x}\delta_{\mathcal{D},x} - cH(x))v^s_x + \omega^2 u^s_{x,0} = -(c - c_{-x}\delta_{\mathcal{D},x} - cH(x))v^i_x \tag{2.7}$$

and

$$c\Delta u^s_{x,-1} - (c - c_{-x}\delta_{\mathcal{D},x} - cH(x))v^s_x + \omega^2 u^s_{x,-1} = (c - c_{-x}\delta_{\mathcal{D},x} - cH(x))v^i_x. \tag{2.8}$$

The skew symmetry follows immediately, i.e.

$$u^s_{x,-1} + u^s_{x,0} = 0, \quad x \in \mathbb{Z}, \tag{2.9}$$

and in general $u^s_{x,-y-1} + u^s_{x,y} = 0$, $y \in \mathbb{Z}^+$. Hence, it is enough to look at $y = 0$, or a difference of equations (2.7) and (2.8). Let $\mathcal{A}$ be an appropriate annulus in the complex plane, the same as that stated in [12], i.e.

$$\mathcal{A} := \{z \in \mathbb{C}: R_+ < |z| < R_-\}, \quad R_+ = \mathrm{e}^{-k_2} \quad \text{and} \quad R_- = \mathrm{e}^{k_2\cos\Theta}. \tag{2.10}$$

Taking into account the skew symmetry of the problem under consideration (see [12] and (2.9)), we conclude that

$$v^F = 2u^F_0. \tag{2.11}$$

Applying the Fourier transform

$$u^F(z) \equiv \sum_{x\in\mathbb{Z}} z^{-x}u^s_x, \quad z \in \mathcal{A}, \tag{2.12}$$

to equation (2.4) for scattering waves in the upper space $y \geq 0$, we obtain, following Slepyan [11] and Sharma [12],

$$u^F_y(z) = \lambda^y(z)u^F_0(z), \quad y = 0, 1, 2, \ldots, \quad z \in \mathcal{A}, \tag{2.13}$$

with

$$\lambda(z) = \frac{r(z) - h(z)}{r(z) + h(z)}, \quad h(z) = \sqrt{Q(z) - 2}, \quad r(z) = \sqrt{Q(z) + 2} \tag{2.14}$$

and

$$Q(z) = 4 - z - z^{-1} - \omega^2. \tag{2.15}$$

An analogous result can be obtained in the lower space ($y \leq -1$). The details are identical to those for a crack without a damage zone as provided in [12].

Taking into account the condition (2.9) as well as (2.13) (in particular, $u_1^F = -u_{-2}^F = u_0^F\lambda$ with λ given by (2.14)), we obtain

$$c\big(\lambda - 1 - Q(z)\big)v^F(z) + 2cv_-(z) - c\mathcal{P}^s(z) = -2cv_-^i(z) + c\mathcal{P}^i(z). \tag{2.16}$$

Thus, with $v^F = v_+ + v_-$, we have

$$(\lambda - Q - 1)(v_+ + v_-) + 2v_- = -2v_-^i + \mathcal{P}^i + \mathcal{P}^s, \tag{2.17}$$

i.e.

$$v_+ + \left(\frac{2}{\lambda - Q - 1} + 1\right)v_- = -\frac{2}{\lambda - Q - 1}v_-^i + \frac{1}{\lambda - Q - 1}\big(\mathcal{P}^i + \mathcal{P}^s\big). \tag{2.18}$$

Simplifying further for $z \in \mathcal{A}$, we get

$$v_+ + Lv_- = (1 - L)v_-^i - \frac{1}{2}(1 - L)\big(\mathcal{P}^i(z) + \mathcal{P}^s(z)\big), \tag{2.19}$$

where $L(z) = h(z)/r(z)$, while $\mathcal{P}^s$ (and $\mathcal{P}^i$) is a polynomial in z given by

$$\mathcal{P}^{s,i}(z) = \frac{2}{c}\sum_{x\in\mathcal{D}} c_{-x}v_x^{s,i}z^{-x}. \tag{2.20}$$

Equation (2.19) is the Wiener–Hopf equation for the Fourier transform of the bonds $v_\pm$ in the cracked row ($x \in \mathbb{Z}^\pm$). Inspection and comparison with the results for a single crack without the damage zone obtained in [12] reveals that the kernel remains the same but there is a presence of an extra unknown polynomial on the right-hand side of the Wiener–Hopf equation.

3. Solution of the Wiener–Hopf equation

The relevant multiplicative factorization of the kernel L in (2.19) on the annulus $\mathcal{A}$, i.e. $L = L_+L_-$, has been obtained in an explicit form in equation (2.27) from [12]. Thus, using this fact, (2.19) can be written as

$$L_+^{-1}v_+ + L_-v_- = \mathtt{C} \quad \text{on } \mathcal{A}, \tag{3.1}$$

where $\mathtt{C} = \mathtt{C}^a + \mathtt{C}^{\mathrm{P}^s}$ and

$$\left.\begin{aligned} &\mathtt{C}^a(z) = (L_+^{-1}(z) - L_-(z))v_-^i(z) \\ \text{and}\quad &\mathtt{C}^{\mathrm{P}}(z) = -\frac{1}{2}(L_+^{-1}(z) - L_-(z))\big(\mathcal{P}^i(z) + \mathcal{P}^s(z)\big). \end{aligned}\right\} \tag{3.2}$$

Note that L_+ is analytic and non-vanishing for $|z| > R_+$ and that L_- is analytic and non-vanishing for $|z| < R_-$. Now

$$v_-^i(z) = A(1 - \mathrm{e}^{ik_y})\delta_{D-}(zz_{\mathsf{P}}^{-1}), \quad z_{\mathsf{P}} = \mathrm{e}^{-ik_x} \tag{3.3}$$

(note that $|z_{\mathsf{P}}| > R_-$ in (2.10)), so that

$$\mathtt{C}^a = \mathtt{C}_+^a + \mathtt{C}_-^a, \tag{3.4}$$

with [12]

$$\mathtt{C}_+^a = \big(L_+^{-1} - L_+^{-1}(z_{\mathsf{P}})\big)v_-^i \quad \text{and} \quad \mathtt{C}_-^a = \big(-L_- + L_+^{-1}(z_{\mathsf{P}})\big)v_-^i. \tag{3.5}$$

Here, $\mathtt{C}_+^a$ is analytic for $|z| > R_+$ and $\mathtt{C}_-^a$ is analytic for $|z| < R_-$. Let $\mathcal{P}^t(z)$ denote the sum $\mathcal{P}^s(z) + \mathcal{P}^i(z)$ (with the coefficients $v_x^t = v_x^s + v_x^i$), i.e.

$$\mathcal{P}^t(z) = \frac{2}{c}\sum_{x\in\mathcal{D}} c_{-x}v_x^t z^{-x}. \tag{3.6}$$

Further (recall that $\mathcal{D}$ is defined in (2.5))

$$L_+^{-1}(z)\mathcal{P}^t(z) = \frac{2}{c}\sum_{x\in\mathcal{D}} c_{-x}v_x^t\left(L_+^{-1}(z)z^{-x}\right), \quad z\in\mathcal{A}. \tag{3.7}$$

Using the expressions from [13], L_+^{-1} can be expanded in a series of the form

$$L_+^{-1}(z) = \sum_{m\in\mathbb{Z}^+} \bar{l}_{+m}z^{-m},$$

for $|z| > R_+$. Thus (with $x = -\nu \in \mathbb{Z}^-$)

$$L_+^{-1}(z)z^{-x} = \sum_{m\in\mathbb{Z}^+} \bar{l}_{+m}z^{-m}z^{\nu} = \phi_+^x(z) + \phi_-^x(z), \quad z\in\mathcal{A}, \tag{3.8}$$

where

$$\phi_+^x(z) = \sum_{m=\nu}^{\infty} \bar{l}_{+m}z^{-m}z^{\nu} \quad \text{and} \quad \phi_-^x(z) = \sum_{m=0}^{\nu-1} \bar{l}_{+m}z^{-m}z^{\nu}, \tag{3.9}$$

and the first term is analytic outside a circle of radius R_+ while the second is analytic inside a circle of radius R_- in the complex plane. Therefore, in the context of (3.7),

$$L_+^{-1}\mathcal{P}^t = \frac{2}{c}\sum_{x\in\mathcal{D}} c_{-x}v_x^t\phi_+^x + \frac{2}{c}\sum_{x\in\mathcal{D}} c_{-x}v_x^t\phi_-^x. \tag{3.10}$$

The above additive splitting of $L_+^{-1}\mathcal{P}^t$, naturally, allows the following additive decomposition:

$$\mathtt{C}^{\mathrm{P}} = \mathtt{C}_+^{\mathrm{P}} + \mathtt{C}_-^{\mathrm{P}} \quad \text{on } \mathcal{A}, \tag{3.11}$$

where

$$\mathtt{C}_+^{\mathrm{P}} = -\frac{1}{c}\sum_{x\in\mathcal{D}} c_{-x}v_x^t\phi_+^x \quad \text{and} \quad \mathtt{C}_-^{\mathrm{P}} = -\frac{1}{c}\sum_{x\in\mathcal{D}} c_{-x}v_x^t\phi_-^x + \frac{1}{2}L_-\mathcal{P}^t, \tag{3.12}$$

which are analytic outside and inside of a circle of radius R_+ and R_- in the complex plane, respectively. As a final step, following the analysis in [12] and using the expressions (3.4), (3.11) and (2.19) leads to

$$\left.\begin{aligned} &L_+^{-1}(z)v_+(z) = \mathtt{C}_+^a(z) + \mathtt{C}_+^{\mathrm{P}}(z) + \chi(z), \quad |z| > R_+, \\ \text{and} \quad &L_-(z)v_-(z) = \mathtt{C}_-^a(z) + \mathtt{C}_-^{\mathrm{P}}(z) - \chi(z), \quad |z| < R_-, \end{aligned}\right\} \tag{3.13}$$

where χ is an arbitrary polynomial in z and z^{-1}. It is shown in [12] that, as $z\to\infty$,

$$L_+^{-1}v_+ - \mathtt{C}_+^a - \mathtt{C}_+^{\mathrm{P}} \to \text{constant},$$

while as $z\to 0$

$$L_-v_- - \mathtt{C}_-^a - \mathtt{C}_-^{\mathrm{P}} \to 0,$$

so that, as a consequence of Liouville's theorem, $\chi \equiv 0$. Hence,

$$\left.\begin{aligned} &v_+(z) = L_+(z)(\mathtt{C}_+^a(z) + \mathtt{C}_+^{\mathrm{P}}(z)), \quad |z| > R_+, \\ \text{and} \quad &v_-(z) = L_-^{-1}(z)(\mathtt{C}_-^a(z) + \mathtt{C}_-^{\mathrm{P}}(z)), \quad |z| < R_-. \end{aligned}\right\} \tag{3.14}$$

Owing to (3.14)

$$\begin{aligned} v^F(z) &= L_+(z)(\mathtt{C}_+^a(z) + \mathtt{C}_+^{\mathrm{P}}(z)) + L_-^{-1}(z)(\mathtt{C}_-^a(z) + \mathtt{C}_-^{\mathrm{P}}(z)) \\ &= v_a^F(z) + v_{\mathrm{P}}^F(z), \quad z\in\mathcal{A}, \end{aligned} \tag{3.15}$$

with

$$v_a^F = L_+\mathtt{C}_+^a + L_-^{-1}\mathtt{C}_-^a \quad \text{and} \quad v_{\mathrm{P}}^F = L_+\mathtt{C}_+^{\mathrm{P}} + L_-^{-1}\mathtt{C}_-^{\mathrm{P}}. \tag{3.16}$$

Also the total field v (the total oscillatory field along the symmetry axis) is given by

$$v_x = v_x^i + v_x^s = v_x^i + \frac{1}{2\pi i}\int_{\mathsf{C}} v^F(z) z^{x-1}\,\mathrm{d}z, \quad x \in \mathbb{Z}. \tag{3.17}$$

In particular, expanding $(3.14)_2$ further,

$$v_- = \left(-1 + L_-^{-1} L_+^{-1}(z_{\mathsf{P}})\right) v_-^i - \frac{1}{c} L_-^{-1} \sum_{x\in\mathcal{D}} c_{-x} v_x^t \phi_-^x + \frac{1}{2}\mathcal{P}^t, \tag{3.18}$$

with $|z| < R_-$. Re-arranging (3.18), we get

$$v_-(z) + v_-^i(z) = L_+^{-1}(z_{\mathsf{P}}) \frac{v_-^i(z)}{L_-(z)} - \frac{1}{c} L_-^{-1}(z) \sum_{x\in\mathcal{D}} c_{-x} v_x^t \phi_-^x(z) + \frac{1}{c}\sum_{x\in\mathcal{D}} c_{-x} v_x^t z^{-x}. \tag{3.19}$$

Let $\mathfrak{P}_{\mathcal{D}}$ denote the projection of Fourier coefficients of a typical $f_-(z)$ for $|z| < R_-$ to the set $\mathcal{D}$, then equation (3.19) leads to

$$\sum_{x\in\mathcal{D}} \left(1 - \frac{c_{-x}}{c}\right) v_x^t z^{-x} + \sum_{x\in\mathcal{D}} \frac{c_{-x}}{c} v_x^t \mathfrak{P}_{\mathcal{D}}\left(\frac{\phi_-^x}{L_-}\right)(z) = \frac{\mathfrak{P}_{\mathcal{D}}\left(\dfrac{v_-^i}{L_-}\right)(z)}{L_+(z_{\mathsf{P}})}, \quad |z| < R_-, \tag{3.20}$$

which yields an $N \times N$ system of linear algebraic equations for $\{v_x^t\}_{\mathcal{D}}$, i.e. the unknowns $\{v_x^s\}_{\mathcal{D}}$, since $\{v_x^i\}_{\mathcal{D}}$ are known in terms of the incident wave (2.2). Indeed, with the notation $\mathfrak{C}_\kappa(p)$ to denote the coefficient of z^κ for polynomials p of the form $\mathfrak{C}_1 z + \mathfrak{C}_2 z^2 + \ldots$, we get

$$\begin{aligned}\sum_{\nu=1}^{N}\left(1 - \frac{c_\nu}{c}\right)\delta_{\kappa\nu} v_{-\nu}^t z^\kappa &+ \sum_{\kappa=1}^{N}\sum_{\nu=1}^{N} \frac{c_\nu}{c} v_{-\nu}^t \mathfrak{C}_\kappa\left(\mathfrak{P}_{\mathcal{D}}\left(\frac{\phi_-^{-\nu}}{L_-}\right)\right) z^\kappa \\ &= L_+^{-1}(z_{\mathsf{P}}) \sum_{\kappa=1}^{N} \mathfrak{C}_\kappa\left(\mathfrak{P}_{\mathcal{D}}\left(\frac{v_-^i}{L_-}\right)\right) z^\kappa, \quad |z| < R_-.\end{aligned} \tag{3.21}$$

The above equation can be written in a symbolic manner as

$$a_{\kappa\nu}\chi_\nu = b_\kappa \qquad (\kappa, \nu = 1, \ldots, N), \tag{3.22}$$

where

$$\left.\begin{aligned} a_{\kappa\nu} &= \left(1 - \frac{c_\nu}{c}\right)\delta_{\kappa\nu} + \frac{c_\nu}{c}\mathfrak{C}_\kappa\left(\mathfrak{P}_{\mathcal{D}}\left(\frac{\phi_-^{-\nu}}{L_-}\right)\right) \\ \text{and} \qquad \chi_\nu &= v_{-\nu}^t, \quad b_\kappa = L_+^{-1}(z_{\mathsf{P}})\mathfrak{C}_\kappa\left(\mathfrak{P}_{\mathcal{D}}\left(\frac{v_-^i}{L_-}\right)\right). \end{aligned}\right\} \tag{3.23}$$

Formally, applying the inversion of the coefficient matrix in (3.22), i.e. $\boldsymbol{\chi} = \mathbf{A}^{-1}\mathbf{b}$, gives $\{v_x^t\}_{x\in\mathcal{D}}$; substitution of this expression back in (3.18), via (3.6), as well as (3.14) leads to the complete solution of the Wiener–Hopf equation. Let $\tilde{a}_{\nu\kappa}$ denote the components of the inverse of $\mathbf{A}$. Then

$$v_x^t = \tilde{a}_{-x\kappa} L_+^{-1}(z_{\mathsf{P}}) \mathfrak{C}_\kappa\left(\mathfrak{P}_{\mathcal{D}}\left(\frac{v_-^i}{L_-}\right)\right). \tag{3.24}$$

The expression (3.24) has been verified using a numerical solution (based on the scheme described in appendix D of [12]) of the discrete Helmholtz equation (2.4) and assumed conditions on the crack faces for several choices of the damaged links; we omit the graphical plots of the comparison as they are indistinguishable on the considered graph scale.

Remark 3.1. When ω_2 $(= \Im\omega)$ is positive, it follows from the Krein conditions that there exists a unique solution in square summable sequences since only a finite number N of damaged links are present. This is a statement on the lines of that provided by Sharma for the sharp crack tip [12,13] and the rigorous results of Ando *et al.* [75]. The limiting case as $N \to \infty$ can be a different story altogether and it is not pursued here.

4. Examples of specific damage zones

Choosing different values of the coefficients $c_{-j}, j \in [1, N]$ one can consider various damage zones. Some of them are discussed below.

(a) Completely destroyed zone

Consider the simplest case when $c_{-x} \equiv 0$. (In fact, it is a bad choice of the left-hand side of the cohesive zone.) Then (3.20) reduces to (using (3.9))

$$\sum_{x\in\mathcal{D}} v_x^t z^{-x} = L_+^{-1}(z_{\mathsf{P}})\mathfrak{P}_{\mathcal{D}}\left(\frac{v_-^i}{L_-}\right)(z), \quad |z| < R_-, \tag{4.1}$$

but $\sum_{x\in\mathcal{D}} v_x^t z^{-x} = \mathfrak{P}_{\mathcal{D}}(v_- + v_-^i)(z)$, so that it is a special case of the complete exact solution given in [12], i.e. $v_-(z) = (L_+^{-1}(z_{\mathsf{P}})L_-^{-1}(z) - 1)v_-^i(z)$, $|z| < R_-$ (see equation (2.29) in [12] and equation (4.1b) in [13]). The detailed analysis and expressions of the solution based on the latter appear in [13], where the single crack was considered. It is natural, as this special case corresponds to a single (slightly longer) crack.

(b) 'Healthy' (no damage) zone

For the case $c_{-x} \equiv c$, the above extra equation (3.20) arises again due to a 'bad choice' of the origin (cohesive crack tip) to define the half-Fourier transforms! Consider the simplest case when $c_{-x} \equiv c$. Evidently, this case coincides with the previous one when $c_{-x} \equiv 0$, except for a shift in the origin from $(0, 0)$ to $(-N, 0)$ (a single slightly shorter crack). Then (3.20) reduces to (using (3.9))

$$\sum_{x\in\mathcal{D}} v_x^t \mathfrak{P}_{\mathcal{D}} L_-^{-1} \sum_{m=0}^{-x-1} \bar{l}_{+m} z^{-m} z^{-x} = L_+^{-1}(z_{\mathsf{P}})\mathfrak{P}_{\mathcal{D}} L_-^{-1} v_-^i, \quad |z| < R_-. \tag{4.2}$$

With the substitution $z \mapsto z^{-1}, x \mapsto -x$ in the above equation, we get

$$\sum_{x=1}^{N} v_{-x}^t \mathfrak{P}_{\mathcal{D}} L_+^{-1}(z) \sum_{m=0}^{x-1} \bar{l}_{+m} z^{m} z^{-x} = L_+^{-1}(z_{\mathsf{P}})\mathfrak{P}_{\mathcal{D}} L_+^{-1}(z) v_-^i(z^{-1}), \quad |z| > R_-^{-1}, \tag{4.3}$$

i.e.

$$\sum_{x=1}^{N} v_{-x}^t \sum_{m=0}^{x-1} \bar{l}_{+m} z^{m} z^{-x} = L_+^{-1}(z_{\mathsf{P}}) v_-^i(z^{-1}), \quad |z| > R_-^{-1}, \tag{4.4}$$

and, finally,

$$\sum_{x=1}^{N} v_{-x}^t z^{-x} L_+^{-1}(z) = L_+^{-1}(z_{\mathsf{P}}) v_-^i(z^{-1}), \quad |z| > R_-^{-1}. \tag{4.5}$$

Here, the reference expression from [12,13] is $v_+ = (1 - L_+^{-1}(z_{\mathsf{P}})L_+)v_-^i, |z| > R_+$, with which it agrees.

(c) A zone with continuously distributed damage

Let us consider a relatively general case that models real damage accumulation in the damage zone. In this case, one can reasonably assume that at the crack tip the stiffness of the interfacial zone is minimal (the damage is most pronounced), then increases monotonically and, finally, at the other end of the zone, it takes the same magnitude as a non-damaged lattice. A typical

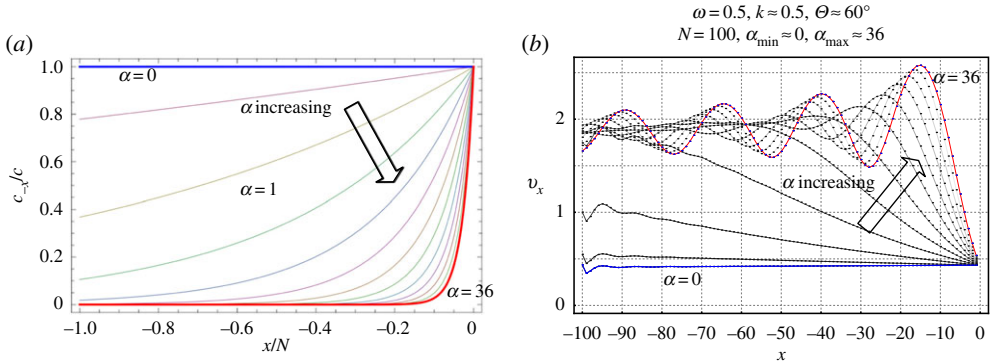

Figure 3. (*a*) Illustration of c_{-x} with $c_{-x} = c\exp(\alpha x/N)$, $x \in \mathcal{D}$. (*b*) Illustration of (total) v_x given by (3.17) for $N = 100$. The curves in blue and red correspond to the minimum and maximum values of α, respectively. (Online version in colour.)

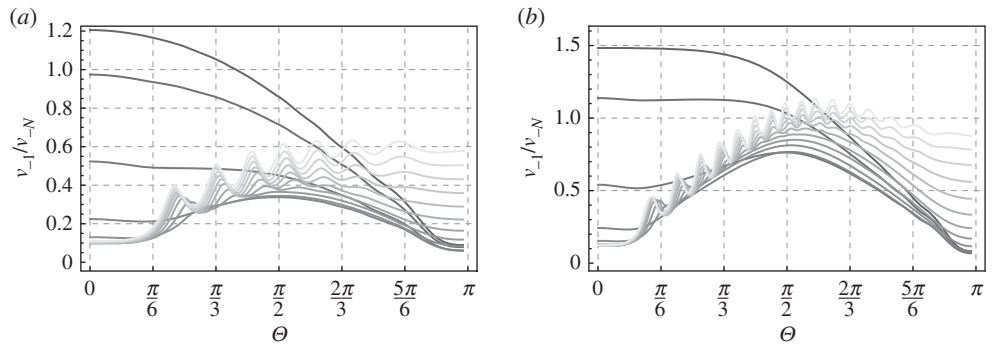

Figure 4. Ratio of the amplitudes at the ends of the damage zone of length $N = 40$. (*a*) corresponds to $\omega = 0.6$. (*b*) represents the other normalized frequency $\omega = 1.2$. Plots for a range of the parameter $\alpha = \{10^{-6}, 0.25, 1, 2.25, 4, 6.25, 9, 12.25, 16, 20.25, 25, 30.3, 36\}$ with a darker shade for smaller α.

representative of such an interface is the exponential distribution

$$c_{-x} = c\exp\left(\frac{\alpha x}{N}\right), \quad x \in \mathcal{D}.$$

The parameter α regulates the rate of damage accumulation. Note that $\alpha \gg 1$ and $\alpha \ll 1$ correspond to part (a) and part (b) of this section, respectively. Figure 3 shows an illustration of v_x^t given by (3.24) for $N = 100$. It is emphasized here that the graphical results for the same choice can be obtained using the numerical scheme (described in appendix D of [12]), and these are found to coincide with the plot in figure 3*b*. As one can see, the presence of a high gradient in the elastic properties of the cohesive zone significantly amplifies the local scattered field near the tip of the zone. As a result, pronounced damage should be expected exactly here that is consistent with the assumptions. However, when α is close enough to zero, the opposite phenomenon happens as now the gradient is small while the jump of the material properties undergoes its maximum value (in fact, it is equivalent to the second case above). It is thus important to compare which part of the damage zone can be subjected to higher risk for further damage. It is also evident that the angle of the incident wave θ may essentially influence the discussed effect. Respective graphical results for the ratio v_{-1}/v_{-N} are presented in figure 4 and show the impact of the incident wave frequency by considering two different normalized values $\omega = 0.6$ and $\omega = 1.2$. As expected large and small values of the parameter α determining the damage gradient inside the zone change the effect significantly. Namely for small values of α the left-hand end of the damage zone is impacted by

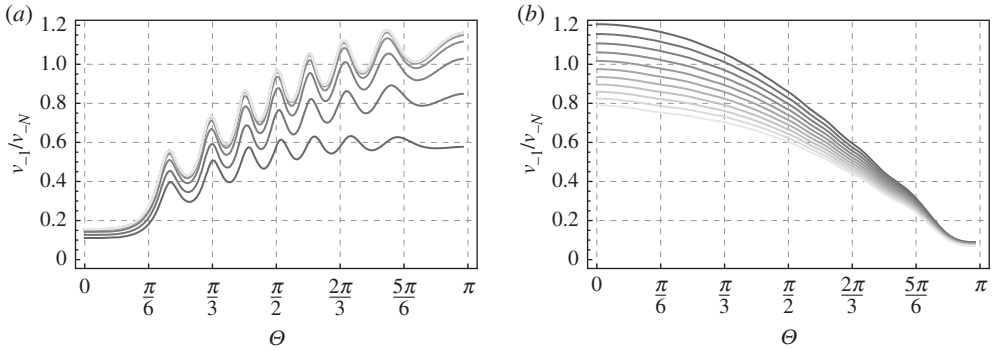

Figure 5. Ratio of the amplitudes at the ends of the damage zone of length $N = 40$ and frequency $\omega = 0.6$. (*a*) corresponds to large values of $\alpha = \{36, 64, 100, 144, 196, 256, 324, 400, 484, 576, 676\}$, while (*b*) corresponds to small values $\alpha = \{10^{-6}, 0.05, 0.1, 0.15, 0.2, 0.25, 0.3, 0.35, 0.4, 0.45, 0.5\}$. Plots for a range of α with a darker shade for smaller α.

higher amplitudes and vice versa. At the right-hand end of the zone (contacting the undamaged part of the zone), the effect is less straightforward. Also for the incident waves parallel to the crack ($\theta = 0$ and $\theta = \pi$) the results are different. The first type can, in fact, be interpreted as the so-called feeding waves (e.g. [30]) for the dynamic case.

In figure 5, we show in more detail the influence of the big and small values of the parameter α. Exact values of the parameters are depicted in the captions of the respective figures.

(d) Damage represented by a bridge crack

Let N be even. In the following, we will use the standard notation:

$$\left.\begin{aligned} &\mathbb{Z}^+ = \{0, 1, 2, \ldots\}, \quad \mathbb{Z}^- = \{-1, -2, \ldots\}, \\ &\mathbb{Z}_e = \{0, \pm 2, \pm 4, \ldots\}, \quad \mathbb{Z}_o = \{\pm 1, \pm 3, \ldots\} \\ \text{and} \quad &\mathbb{Z}_S^- = \mathbb{Z}_- \backslash \mathcal{D}, \quad \mathbb{Z}_S^+ = \mathbb{Z}_+ \cup \mathcal{D}, \end{aligned}\right\} \tag{4.6}$$

for different subsets of the set of entire numbers. Consider the case when

$$c_{-x} = c, \quad x \in \mathcal{D} \cap \mathbb{Z}_e \quad \text{and} \quad c_{-x} = 0, \quad x \in \mathcal{D} \cap \mathbb{Z}_o$$

(figure 6). Here, $\max |\mathcal{D} \cap \mathbb{Z}_e|$ is N, which is replaced by $2M$ for convenience; thus the intact bonds on the even sites in the cracked row begin at $x = -2M$. The difference between (2.7) and (2.8) becomes

$$\begin{aligned} &c(2u^s_{x,1} + v^s_{x+1,0} + v^s_{x-1,0} + (-5 + \omega^2)v^s_{x,0}) + 2\Big(c - cH(x + 2M)\delta_{x,e} - cH(x)\delta_{x,o}\Big)v^s_x \\ &\quad = -2\Big(c - cH(x + 2M)\delta_{x,e} - cH(x)\delta_{x,o}\Big)v^i_x. \end{aligned} \tag{4.7}$$

Using the Fourier transform (2.12) to equation (4.7) and taking into account the following representations of the functions $u^F(z) = (u^s_x)^F$, $v^F(z) = (v^s_x)^F$:

$$u^F(z) \equiv u^+(z) + u^-(z), \quad u^\pm(z) = \sum_{\mathbb{Z}^\pm} z^{-x} u_x, \quad z \in \mathcal{A}, \tag{4.8}$$

$$v^F(z) = v^+(z) + v^-(z), \quad v^\pm(z) = z^{2M} v^\pm_e(z) + v^\pm_o(z), \tag{4.9}$$

$$v^\pm_e(z) = z^{-2M} \sum_{\mathbb{Z}_S^\pm \cap \mathbb{Z}_e} z^{-x} v_x = \sum_{\mathbb{Z}^\pm \cap \mathbb{Z}_e} z^{-x} v_x, \quad z \in \mathcal{A} \tag{4.10}$$

and

$$v^\pm_o(z) = \sum_{\mathbb{Z}^\pm \cap \mathbb{Z}_o} z^{-x} v_x, \quad z \in \mathcal{A}, \tag{4.11}$$

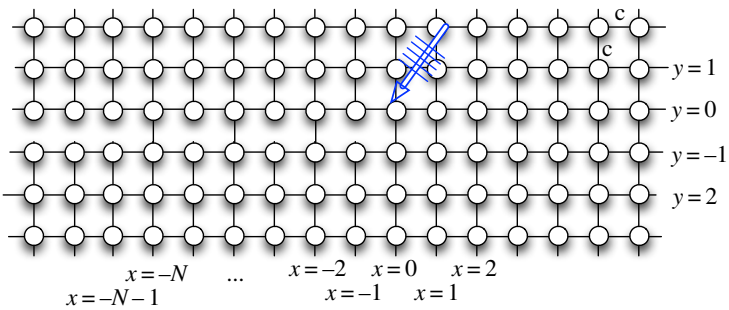

Figure 6. Geometry of the square lattice structure with a partially open crack tip and $N = 2$ and $M = 6$. (Online version in colour.)

we get

$$d^{-1}(z) = \lambda(z) - 1 - Q(z) = -(\lambda^{-1} + 1) \tag{4.12}$$

and

$$d(z)^{-1}(z^{2M}v_{\mathrm{e}}^{+} + v_{o}^{+} + z^{2M}v_{\mathrm{e}}^{-} + v_{o}^{-}) + 2(z^{2M}v_{\mathrm{e}}^{-} + v_{o}^{-}) = -2(z^{2M}v_{\mathrm{e}}^{i-} + v_{o}^{i-}), \tag{4.13}$$

where we have taken into account that $z \mapsto -z$, since $v_{\mathrm{e}}^{+}(z) = v_{\mathrm{e}}^{+}(-z)$ while $v_{o}^{+}(z) = -v_{o}^{+}(-z)$. Thus, we obtain the matrix Wiener–Hopf equation

$$\mathbf{A}(z)\mathbf{v}^{+}(z) + \mathbf{B}(z)\mathbf{v}^{-}(z) = \mathbf{f}(z), \quad z \in \mathcal{A}, \tag{4.14}$$

where we have defined new plus and minus vector functions $\mathbf{v}^{\pm}(z) = (v_{e}^{\pm}, v_{o}^{\pm})^{\top}$. The components of the matrices $\mathbf{A}(s)$, $\mathbf{B}(s)$ and the right-hand side of equation (4.14) are

$$\begin{aligned} &a_{11} = 1, \quad b_{11} = (1 + 2d(z)), \quad a_{12}(z) = z^{-2M}, \quad b_{12}(z) = z^{-2M}(1 + 2d(z)), \\ &a_{21} = z^{2M}, \quad b_{21} = z^{2M}(1 + 2d(-z)), \quad a_{22}(z) = -1, \quad b_{22}(z) = -(1 + 2d(-z)) \end{aligned} \tag{4.15}$$

and

$$f_1(z) = -2(v_{\mathrm{e}}^{i-} - z^{-2M}v_{o}^{i-})d(z), \quad f_2(z) = -2(z^{2M}v_{\mathrm{e}}^{i-} + v_{o}^{i-})d(-z), \tag{4.16}$$

where $d(z)$ has already been defined in (4.12). Note $\mathbf{B} = \mathbf{A} + \mathbf{D}$, $d_{11} = 2d(z)$, $d_{12} = z^{-2M}2d(z)$, $d_{21} = z^{2M}2d(-z)$, $d_{22} = -2d(-z)$. Let

$$\begin{aligned} \mathbf{C} = \mathbf{I} + \mathbf{A}^{-1}\mathbf{D} &= \mathbf{I} + \frac{1}{\det \mathbf{A}} \begin{pmatrix} a_{22} & -a_{12} \\ -a_{21} & a_{11} \end{pmatrix} \begin{pmatrix} d_{11} & d_{12} \\ d_{21} & d_{22} \end{pmatrix} \\ &= \mathbf{I} - \begin{pmatrix} d(z) & 0 \\ 0 & -d(-z) \end{pmatrix} \begin{pmatrix} 1 & z^{-2M} \\ -z^{2M} & 1 \end{pmatrix} = \begin{pmatrix} 1 - d(z) & -d(z)z^{-2M} \\ -d(-z)z^{2M} & 1 + d(-z) \end{pmatrix}. \end{aligned} \tag{4.17}$$

Equation (4.14) can be rewritten in an equivalent form

$$\mathbf{v}^{+}(z) + \mathbf{C}(z)\mathbf{v}^{-}(z) = \mathbf{A}^{-1}(z)\mathbf{f}(z), \quad z \in \mathcal{A}, \tag{4.18}$$

where $\mathbf{C}(z) = \mathbf{A}^{-1}(z)\mathbf{B}(z)$. The matrix $\mathbf{C}$ possesses a structure which in general does not admit factorization by standard techniques for arbitrary N (for $N = 1$, perhaps).

On the other hand, as has been proven above, this special case can be reduced to the solution of N linear algebraic equations (see also [56]). For example, the problem with a cohesive zone of similar geometry in *continuous formulation* [76] cannot be reduced to a scalar Wiener–Hopf problem and requires an application of other numerical techniques [57,71,72,77].

In figure 7, we show the ratio of amplitudes in the last two points on the left-hand side of the damage zone to that on the right-hand side of the zone ($x = 0$). Exact values of the parameters are depicted in the captions of the respective figures. Now we examine in more detail the impact of the frequency of the incident waves.

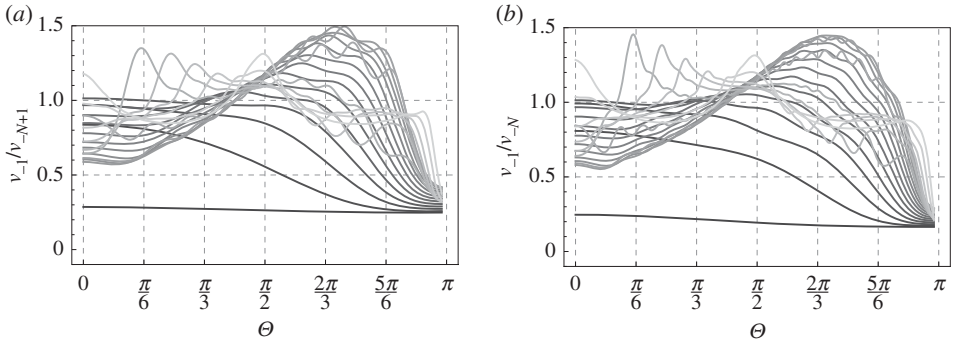

Figure 7. Length of the damage zone: $N = 40$. Bridged bonds are $x = -1, -3, \ldots, -N+1$ and bonds intact: $x = -2, -4, \ldots, -N$. Plots for a range of frequencies of the incident waves: $\omega = \{0.01, 0.1, 0.2, 0.3, 0.4, 0.5, 0.6, 0.7, 0.8, 0.9, 1.0, 1.1, 1.2, 1.3, 1.4, 1.5, 1.6, 1.7, 1.8, 1.9, 1.95\}$, with a darker shade used for smaller ω.

In the context of the matrix kernel (4.17), with the distinguished presence of the off-diagonal factors z^{-2M} and z^{2M}, the reduction to the linear algebraic equation obtained above is reminiscent of that proposed for the Wiener–Hopf kernel with exponential phase factors that appear in several continuum scattering problems in fluid mechanics and fracture mechanics [52–55], and their discrete analogues in the form of scattering due to a pair of staggered cracks and rigid constraints [34,56,78]; both of these are based on an exact solution of the corresponding staggerless case [35,79–81].

5. Reconstruction of the scattered field

Let C be a contour in the annulus $\mathcal{A}$. By the inverse Fourier transform $u^s_{x,y} = (1/2\pi i)\int_{\mathsf{C}} u^F_y(z) z^{x-1}\,\mathrm{d}z$, i.e.

$$u^s_{x,y} = \frac{1}{2\pi i}\frac{1}{2}\int_{\mathsf{C}} v^F(z)\lambda^y(z) z^{x-1}\,\mathrm{d}z, \quad x \in \mathbb{Z}, \quad y = 0, 1, 2, \ldots, \tag{5.1}$$

where v^F is given by (3.15). For $y = 0, 1, 2, \ldots, u^s_{x,-y-1} = -u^s_{x,y}$, $x \in \mathbb{Z}$, due to skew symmetry. The total wave field is given by

$$u_{x,y} = u^s_{x,y} + u^i_{x,y}, \quad x \in \mathbb{Z}, \quad y \in \mathbb{Z}. \tag{5.2}$$

Concerning the effect of the damage, using the decomposition $v^F(z) = v^F_a(z) + v^F_{\mathrm{P}}(z)$ (3.15), it is easy to see that $v^F_a(z)$ coincides with the solution given in [12], i.e. it describes the scattering due to an undamaged crack tip; thus, the effect of the damage zone is represented by the second term $v^F_{\mathrm{P}}(z)$ in (3.15).

The perturbation in the scattered field (5.1) induced by the damage zone is given by

$$\begin{aligned}
\hat{u}_{x,y} &= \frac{1}{2\pi i}\frac{1}{2}\int_{\mathsf{C}} v^F_{\mathrm{P}}(z)\lambda^y(z) z^{x-1}\,\mathrm{d}z, \quad x \in \mathbb{Z}, \quad y = 0, 1, 2, \ldots, \\
&= \frac{1}{2\pi i}\frac{1}{2}\int_{\mathsf{C}} (L_+\mathsf{C}^{\mathrm{P}}_+ + L_-^{-1}\mathsf{C}^{\mathrm{P}}_-)\lambda^y(z) z^{x-1}\,\mathrm{d}z \\
&= \frac{1}{2\pi i}\frac{1}{2}\int_{\mathsf{C}} \left(-\frac{1}{c}\sum_{m\in\mathcal{D}} c_{-m} v^t_m (L_+\phi^m_+ + L_-^{-1}\phi^m_-) + \frac{1}{c}\sum_{m\in\mathcal{D}} c_{-m} v^t_m z^{-m}\right)\lambda^y(z) z^{x-1}\,\mathrm{d}z \\
&= \frac{1}{2L_+(z_{\mathrm{P}})}\sum_{m\in\mathcal{D}} \frac{c_{-m}}{c}\tilde{a}_{-m\kappa}\mathfrak{C}_\kappa\left(\mathfrak{P}_{\mathcal{D}}\frac{v^i_-}{L_-}\right)\frac{1}{2\pi i}\int_{\mathsf{C}} \Lambda_m(z)\lambda^y(z) z^{x-1}\,\mathrm{d}z,
\end{aligned} \tag{5.3}$$

where

$$\Lambda_m(z) = z^{-m} - (L_+(z)\phi^m_+(z) + L_-^{-1}(z)\phi^m_-(z)), \quad m \in \mathcal{D}. \tag{5.4}$$

For $\xi\sqrt{x^2+y^2} \gg 1$ and $\omega/c \in (0,2)$, where $\xi \sim \omega/c$ is related to the wavenumber of an incident wave, a far-field approximation of the exact solution (5.1) can be constructed; also an analogous result holds for $\omega/c \in (2, 2\sqrt{2})$. It is sufficient for our purposes to focus on the effect of the damage zone $\mathcal{D}$ so that we investigate the far-field approximation of (5.3), i.e. mainly associated with the expression of Λ_m given by (5.4) for each $m \in \mathcal{D}$. Following [12], the approximation of the far field can be obtained using the stationary phase method [82]. The substitution $z = \mathrm{e}^{-i\xi}$ maps the contour $\mathtt{C}$ into a contour C_ξ. In terms of polar coordinates (R, θ), the lattice point (x, y) can be expressed as

$$x = R\cos\theta, y = R\sin\theta. \tag{5.5}$$

Let

$$\Phi(\xi) = \eta(\xi)\sin\theta - \xi\cos\theta, \eta(\xi) = -i\log\lambda(\mathrm{e}^{-i\xi}). \tag{5.6}$$

The function Φ (5.6) possesses a saddle point [83,84] at $\xi = \xi_S$ on C_ξ, with $\Phi'(\xi_S) = \eta'(\xi_S)\sin\theta - \cos\theta = 0, \Phi''(\xi_S) = \eta''(\xi_S)\sin\theta \neq 0$, which is the same as that discussed in [12]. Omitting the details of the calculations, it is found that

$$\hat{u}_{x,y} \sim \frac{1}{2\sqrt{\pi}} \frac{1 + i\,\mathrm{sign}(\eta''(\xi_S))}{2c} \frac{\lambda^y(\mathrm{e}^{-i\xi_S})\mathrm{e}^{-i\xi_S(x-1)}}{(R|\eta''(\xi_S)|\sin\theta)^{1/2}} \sum_{m\in\mathcal{D}} (c_{-m} v_m^t \Lambda_m(\mathrm{e}^{-i\xi_S})), \tag{5.7}$$

as $\omega R/c \to \infty$. The expression (5.7) has been verified using a numerical solution of the discrete Helmholtz equation (based on the scheme described in appendix D of [12]); a graphical demonstration of the same is omitted in the paper.

6. Concluding remarks

We have shown how the scattering problem in a square lattice with an infinite crack with a damage zone near the crack tip of arbitrary properties can be effectively solved by We were able to reduce it to a scalar Wiener–Hopf method. We have applied a new method that uses specific discrete properties of the system under consideration. It consists of solving an auxiliary $N \times N$ system of linear equations with a unique solution (remark 3.1). The effectiveness of the method has been highlighted by some numerical examples and the constructed asymptotic expression of the scattered field at infinity. Analysis of the solution near two ends of the damage zone and at infinity can be used in a non-destructive testing procedure, among other applications. The method may be useful for solving other matrix Wiener–Hopf problems appearing in the analysis of the dynamics of discrete structures with defects. Indeed, the discrete scattering problem for the bridge damage zone has been written in a vectorial problem with a 2×2 matrix-kernel and has simultaneously transformed it, by the aforementioned approach, to a scalar one (modulo the accompanying linear algebraic equation). This gives rise for a hope for building a closed form standard procedure that allows for effective factorization of similar matrices of an arbitrary size.

Data accessibility. There are no data in the paper. All the plots are based on expressions provided and are not dependent on a numerical code/software.

Authors' contributions. Both authors contributed equally to the writing of the manuscript, the problem formulation as well as the discussion/interpretation of the results in the context of special cases of the damage zone. The Wiener–Hopf analysis and the technique of reduction to a linear algebraic equation as well as the asymptotic approximation of the scattered field is due to B.L.S., in addition to the numerical calculations based on the semi-analytical approach and a direct numerical solution of the scattering problem. The formulation of the bridged crack and the relationship of the scattering problem to the 2×2 matrix kernels is due to G.M.

Competing interests. We declare we have no competing interest.

Funding. B.L.S. acknowledges the partial support of SERB MATRICS grant no. MTR/2017/000013. G.M. acknowledges financial support from the ERC Advanced Grant 'Instabilities and nonlocal multiscale modelling of materials', ERC-2013-ADG-340561-INSTABILITIES. He is also thankful to the Royal Society for the Wolfson Research Merit Award and the Isaac Newton Institute for Mathematical Sciences for the Simon Fellowship. This programme was supported by EPSRC grant no. EP/R014604/1.

Acknowledgements. The authors thank the Isaac Newton Institute for Mathematical Sciences, Cambridge, UK, for support and hospitality during the programme 'Bringing pure and applied analysis together via the Wiener–Hopf technique, its generalizations and applications', where work on this paper was completed.

References

1. Chadwick P. 1999 *Continuum mechanics: concise theory and problems*. New York, NY: Dover.
2. Chadwick P, Powdrill B. 1964 Application of the Laplace transform method to wave motions involving strong discontinuities. *Math. Proc. Camb. Philos. Soc.* **60**, 313–324. (doi:10.1017/S0305004100037786)
3. Chadwick P, Seet L. 1970 Wave propagation in a transversely isotropic heat-conducting elastic material. *Mathematika* **17**, 255–274. (doi:10.1112/S002557930000293X)
4. Chadwick P, Smith G. 1977 Foundations of the theory of surface waves in anisotropic elastic materials. In *Advances in applied mechanics*, vol. 17, pp. 303–376. New York, NY: Elsevier.
5. Chadwick P, Smith G. 1982 Surface waves in cubic elastic materials. In *Mechanics of solids*, pp. 47–100. Oxford, UK: Elsevier.
6. Chadwick P. 1989 Wave propagation in transversely isotropic elastic media-i. Homogeneous plane waves. *Proc. R. Soc. Lond. A* **422**, 23–66. (doi:10.1098/rspa.1989.0019)
7. Chadwick P, Whitworth A, Borejko P. 1987 Basic theory of small-amplitude waves in a constrained elastic body. In *Analysis and thermomechanics*, pp. 65–80. New York, NY: Springer.
8. Chadwick P. 1997 The application of the Stroh formalism to prestressed elastic media. *Math. Mech. Solids* **2**, 379–403. (doi:10.1177/108128659700200402)
9. Slepyan LI. 1981 Dynamics of a crack in a lattice. *Doklady Soviet Phys.* **26**, 538–540.
10. Slepyan LI. 1982 Antiplane problem of a crack in a lattice. *Mech. Solids* **17**, 101–114.
11. Slepyan LI. 2002 *Models and phenomena in fracture mechanics*. Berlin, Germany: Springer.
12. Sharma BL. 2015 Diffraction of waves on square lattice by semi-infinite crack. *SIAM J. Appl. Math.* **75**, 1171–1192. (doi:10.1137/140985093)
13. Sharma BL. 2015 Near-tip field for diffraction on square lattice by crack. *SIAM J. Appl. Math.* **75**, 1915–1940. (doi:10.1137/15M1010646)
14. Sharma BL. 2016 Wave propagation in bifurcated waveguides of square lattice strips. *SIAM J. Appl. Math.* **76**, 1355–1381. (doi:10.1137/15M1051464)
15. Born M, Huang K. 1985 *Dynamical theory of crystal lattices*. The International Series of Monographs on Physics. Oxford Classic Texts in the Physical Sciences. Oxford, UK: Oxford University Press, The Clarendon Press.
16. Atkinson W, Cabrera N. 1965 Motion of a Frenkel-Kontorowa dislocation in a one-dimensional crystal. *Phys. Rev.* **138**, A763–A766. (doi:10.1103/PhysRev.138.A763)
17. Celli V, Flytzanis N. 1970 Motion of a screw dislocation in a crystal. *J. Appl. Phys.* **41**, 4443–4447. (doi:10.1063/1.1658479)
18. Thomson R, Hsieh C, Rana V. 1971 Lattice trapping of fracture cracks. *J. Appl. Phys.* **42**, 3154–3160. (doi:10.1063/1.1660699)
19. Slepyan LI. 2000 Dynamic factor in impact, phase transition and fracture. *J. Mech. Phys. Solids* **48**, 927–960. (doi:10.1016/S0022-5096(99)00061-7)
20. Kulakhmetova S, Saraikin V, Slepyan L. 1984 Plane problem of a crack in a lattice. *Mech. Solids* **19**, 101–108.
21. Marder M. 2004 Effects of atoms on brittle fracture. *Int. J. Fract.* **130**, 517–555. (doi:10.1023/B:FRAC.0000049501.35598.87)
22. Marder M, Gross S. 1995 Origin of crack tip instabilities. *J. Mech. Phys. Solids* **43**, 1–48. (doi:10.1016/0022-5096(94)00060-I)
23. Slepyan L. 2001 Feeding and dissipative waves in fracture and phase transition. I. Some 1D structures and a square-cell lattice. *J. Mech. Phys. Solids* **49**, 25–67. (doi:10.1016/S0022-5096(00)00064-8)
24. Slepyan L. 2001 Feeding and dissipative waves in fracture and phase transition. II. Phase-transition waves. *J. Mech. Phys. Solids* **49**, 69–106. (doi:10.1016/S0022-5096(00)00064-8)
25. Slepyan L. 2001 Feeding and dissipative waves in fracture and phase transition. III. Triangular-cell lattice. *J. Mech. Phys. Solids* **49**, 2839–2875. (doi:10.1016/S0022-5096(01)00053-9)
26. Movchan A, Slepyan L. 2007 Band gap Green's functions and localized oscillations. *Proc. R. Soc. A* **463**, 2709–2727. (doi:10.1098/rspa.2007.0007)

27. Mishuris GS, Movchan AB, Slepyan LI. 2007 Waves and fracture in an inhomogeneous lattice structure. *Waves Random Complex Media* **17**, 409–428. (doi:10.1080/17455030701459910)
28. Mishuris G, Movchan A, Slepyan L. 2008 Dynamics of a bridged crack in a discrete lattice. *Q. J. Mech. Appl. Math.* **61**, 151–160. (doi:10.1093/qjmam/hbm030)
29. Ayzenberg-Stepanenko M, Slepyan L. 2008 Resonant-frequency primitive waveforms and star waves in lattices. *J. Sound Vib.* **313**, 812–821. (doi:10.1016/j.jsv.2007.11.047)
30. Mishuris G, Movchan A, Slepyan L. 2009 Localised knife waves in a structured interface. *J. Mech. Phys. Solids* **57**, 1958–1979. (doi:10.1016/j.jmps.2009.08.004)
31. Slepyan L. 2010 Wave radiation in lattice fracture. *Acoust. Phys.* **56**, 962–971. (doi:10.1134/S1063771010060217)
32. Sharma BL. 2016 On energy balance and the structure of radiated waves in kinetics of crystalline defects. *J. Mech. Phys. Solids* **96**, 88–120. (doi:10.1016/j.jmps.2016.05.036)
33. Colquitt D, Nieves M, Jones I, Movchan A, Movchan N. 2013 Localization for a line defect in an infinite square lattice. *Proc. R. Soc. A* **469**, 2012057. (doi:10.1098/rspa.2012.0579)
34. Maurya G, Sharma BL. 2019 Scattering by two staggered semi-infinite cracks on square lattice: an application of asymptotic Wiener–Hopf factorization. *Z. Angew. Math. Phys.* **70**, 133. (doi:10.1007/s00033-019-1183-2)
35. Sharma BL, Maurya G. 2019 Discrete scattering by a pair of parallel defects. *Phil. Trans. R. Soc. A* **378**, 1–20.
36. Sharma BL. 2017 On scattering of waves on square lattice half-plane with mixed boundary condition. *Z. Angew. Math. Phys.* **68**, 120. (doi:10.1007/s00033-017-0854-0)
37. Sharma BL. 2015 Diffraction of waves on square lattice by semi-infinite rigid constraint. *Wave Motion* **59**, 52–68. (doi:10.1016/j.wavemoti.2015.07.008)
38. Sharma BL. 2016 Diffraction of waves on triangular lattice by a semi-infinite rigid constraint and crack. *Int. J. Solids Struct.* **80**, 465–485. (doi:10.1016/j.ijsolstr.2015.10.008)
39. Sharma BL. 2016 Edge diffraction on triangular and hexagonal lattices: existence, uniqueness, and finite section. *Wave Motion* **65**, 55–78. (doi:10.1016/j.wavemoti.2016.04.005)
40. Sharma BL. 2015 Discrete Sommerfeld diffraction problems on hexagonal lattice with a zigzag semi-infinite crack and rigid constraint. *Z. Angew. Math. Phys.* **66**, 3591–3625. (doi:10.1007/s00033-015-0574-2)
41. Movchan A, Movchan N, Jones I, Colquitt D. 2017 *Mathematical modelling of waves in multi-scale structured media*. Providence, RI: CRC Press.
42. Sharma BL, Eremeyev VA. 2019 Wave transmission across surface interfaces in lattice structures. *Int. J. Eng. Sci.* **145**, 103173. (doi:10.1016/j.ijengsci.2019.103173)
43. Sharma BL. 2017 Continuum limit of discrete Sommerfeld problems on square lattice. *Sādhanā* **42**, 713–728. (doi:10.1007/s12046-017-0636-6)
44. Sommerfeld A. 2004 *Mathematical theory of diffraction*, vol. 35. Progress in Mathematical Physics. Boston, MA: Birkhäuser.
45. Sommerfeld A. 1896 Mathematische theorie der diffraction. *Math. Ann.* **47**, 317–374. (doi:10.1007/BF01447273)
46. Dugdale DS. 1960 Yielding of steel sheets containing slits. *J. Mech. Phys. Solids* **8**, 100–104. (doi:10.1016/0022-5096(60)90013-2)
47. Barenblatt GI. 1962 The mathematical theory of equilibrium cracks in brittle fracture. In *Advances in applied mechanics*, vol. 7, pp. 55–129. New York, NY: Elsevier.
48. Cox B, Marshall D. 1994 Concepts for bridged cracks in fracture and fatigue. *Acta Metall. Mater.* **42**, 341–363. (doi:10.1016/0956-7151(94)90492-8)
49. Gorbushin N, Vitucci G, Volkov G, Mishuris G. 2018 Influence of fracture criteria on dynamic fracture propagation in a discrete chain. *Int. J. Fracture* **209**, 131–142. (doi:10.1007/s10704-017-0246-7)
50. Nieves MJ, Mishuris GS, Slepyan LI. 2017 Transient wave in a transformable periodic flexural structure. *Int. J. Solids Struct.* **112**, 185–208. (doi:10.1016/j.ijsolstr.2016.11.012)
51. Noble B. 1958 *Methods based on the Wiener-Hopf technique for the solution of partial differential equations*, vol. 7. International Series of Monographs on Pure and Applied Mathematics. New York, NY: Pergamon Press.
52. Abrahams ID, Wickham GR. 1990 General Wiener-Hopf factorization of matrix kernels with exponential phase factors. *SIAM J. Appl. Math.* **50**, 819–838. (doi:10.1137/0150047)
53. Abrahams ID, Wickham GR. 1988 On the scattering of sound by two semi-infinite parallel staggered plates. I. Explicit matrix Wiener-Hopf factorization. *Proc. R. Soc. Lond.* **420**, 131–156. (doi:10.1098/rspa.1988.0121)

54. Abrahams ID, Wickham GR. 1990 The scattering of sound by two semi-infinite parallel staggered plates. II. Evaluation of the velocity potential for an incident plane wave and an incident duct mode. *Proc. R. Soc. Lond. A* **427**, 139–171. (doi:10.1098/rspa.1990.0006)
55. Abrahams ID, Wickham GR. 1990 Acoustic scattering by two parallel slightly staggered rigid plates. *Wave Motion* **12**, 281–297. (doi:10.1016/0165-2125(90)90044-5)
56. Sharma BL. 2019 Discrete scattering by two staggered semi-infinite defects: reduction of matrix Wiener–Hopf problem. (http://arxiv.org/abs/1908.11804), 1–20.
57. Mishuris G, Rogosin S. 2014 An asymptotic method of factorization of a class of matrix functions. *Proc. R. Soc. A* **470**, 20140109. (doi:10.1098/rspa.2014.0109)
58. Heins AE, Silver S. 1965 The edge conditions and field representation theorems in the theory of electromagnetic diffraction. *Proc. Camb. Phil. Soc.* **51**, 149–161. (doi:10.1017/S0305004100030036)
59. Morse PM, Feshbach H. 1953 *Methods of theoretical physics*, vol. 2. New York, NY: McGraw-Hill Book Co., Inc.
60. Paley REAC, Wiener N. 1934 *Fourier transforms in the complex domain*. Providence, RI: American Mathematical Society.
61. Wiener N, Hopf E. 1931 Über eine Klasse singulärer Integralgleichungen. *Sitzungsber. Preuss. Akad. Wiss. Berlin, Phys.-Math.* **32**, 696–706.
62. Mikhlin SG, Prößdorf S. 1986 *Singular integral operators*. Berlin, Germany: Springer-Verlag.
63. Gakhov FD. 1990 *Boundary value problems*. New York, NY: Dover Publications, Inc. Translated from the Russian. Reprint of the 1966 translation.
64. Titchmarsh EC. 1986 *Introduction to the theory of Fourier integrals*, 3rd edn. New York, NY: Chelsea Publishing Co.
65. Gohberg I, Krein MG. 1960 System of integral equations on a half-plane with kernels depending on the difference of arguments. *Am. Math. Soc. Transl. Ser. 2* **14**, 217–287.
66. Bottcher A, Silbermann B. 2006 *Analysis of Toeplitz operators*, 2nd edn. Cambridge, UK: Springer.
67. Prößdorf S, Speck FO. 1990 A factorisation procedure for two by two matrix functions on the circle with two rationally independent entries. *Proc. R. Soc. Edinb.: Sect. A Math.* **115**, 119–138. (doi:10.1017/S0308210500024616)
68. Meister E, Rottbrand K. 1996 Elastodynamical scattering by N parallel half-planes in $\mathbf{R}^3$. *Math. Nachr.* **177**, 189–232. (doi:10.1002/mana.19961770112)
69. Meister E, Rottbrand K. 1997 Elastodynamical scattering by N parallel half-planes in $\mathbf{R}^3$. II. Explicit solutions for $N = 2$ by explicit symbol factorization. *Integr. Equ. Oper. Theory* **29**, 70–109. (doi:10.1007/BF01191481)
70. Daniele V. 1984 On the solution of two coupled Wiener–Hopf equations. *SIAM J. Appl. Math.* **44**, 667–680. (doi:10.1137/0144048)
71. Mishuris G, Rogosin S. 2016 Factorization of a class of matrix-functions with stable partial indices. *Math. Methods Appl. Sci.* **39**, 3791–3807. (doi:10.1002/mma.3825)
72. Rogosin S, Mishuris G. 2016 Constructive methods for factorization of matrix-functions. *IMA J. Appl. Math.* **81**, 365–391. (doi:10.1093/imamat/hxv038)
73. Mishuris G, Rogosin S. 2018 Regular approximate factorization of a class of matrix-function with an unstable set of partial indices. *Proc. R. Soc. A* **474**, 20170279. (doi:10.1098/rspa.2017.0279)
74. Collatz L. 1960 *The numerical treatment of differential equations*, 3rd edn. Berlin, Germany: Springer.
75. Ando K, Isozaki H, Morioka H. 2015 Spectral properties of Schrödinger operators on perturbed lattices. https://arxiv.org/pdf/1408.2076.pdf.
76. Livasov P, Mishuris G. 2019 Numerical factorization of a matrix-function with exponential factors in an anti-plane problem for a crack with process zone. *Phil. Trans. R. Soc. A* **377**, 20190109. (doi:10.1098/rsta.2019.0109)
77. Kisil A. 2018 An iterative Wiener–Hopf method for triangular matrix functions with exponential factors. *SIAM J. Appl. Math.* **78**, 45–62. (doi:10.1137/17M1136304)
78. Maurya G. 2019 On some problems involving multiple scattering due to edges. PhD thesis, Indian Institute of Technology Kanpur, Kanpur, India.
79. Heins AE. 1948 The radiation and transmission properties of a pair of semi-infinite parallel plates. I. *Q. Appl. Math.* **6**, 157–166. (doi:10.1090/qam/25981)
80. Heins AE. 1948 The radiation and transmission properties of a pair of semi-infinite parallel plates. II. *Q. Appl. Math.* **6**, 215–220. (doi:10.1090/qam/26922)

81. Abrahams I, Wickham G. 1990 Acoustic scattering by two parallel slightly staggered rigid plates. *Wave Motion* **12**, 281–297. (doi:10.1016/0165-2125(90)90044-5)
82. Felsen LB, Marcuvitz N. 1973 *Radiation and scattering of waves*. Prentice-Hall Microwaves and Fields Series. Englewood Cliffs, NJ: Prentice-Hall, Inc.
83. Erdélyi A. 1955 Asymptotic representations of Fourier integrals and the method of stationary phase. *J. Soc. Ind. Appl. Math.* **3**, 17–27. (doi:10.1137/0103002)
84. Felsen LB, Marcuvitz N. 1973 *Radiation and scattering of waves*. Englewood Cliffs, NJ: Prentice-Halls.